scientific reports

Check for updates

OPEN

Microplastic exposure linked to accelerated aging and impaired adipogenesis in fat cells

Hanbyeol Moon[1,6], Damin Jeong[2,6], Jung-Won Choi[3], Seongtae Jeong[4], Hojin Kim[5], Byeong-Wook Song[2,3], Soyeon Lim[2,3], Il-Kwon Kim[2,3], Seahyoung Lee[2,3] & Sang Woo Kim[2,3]✉

Our research explores the detrimental effects of microplastic (MP) exposure on adipose tissue aging and function, emphasizing the potential health risks associated with environmental pollutants. Utilizing both in vivo and in vitro models, we discovered that MPs accumulate in adipose tissues, leading to cellular senescence, inflammation, and hindered adipogenic differentiation. Notably, our findings demonstrate that MPs prompt an aging response in both epididymal and inguinal white adipose tissue, increase senescence-associated β-galactosidase activity, and upregulate key senescence and inflammatory markers. Furthermore, we show that MPs disrupt normal adipogenic differentiation by reducing lipid droplet formation and downregulating critical adipogenic markers. These insights highlight the urgent need for further investigation into the long-term consequences of MP pollution on biological aging and underscore the importance of developing public health strategies to mitigate these effects.

Keywords Adipose tissue, Differentiation, Inflammation, Microplastic, Senescence

In the modern era, the proliferation of plastics has led to the inadvertent seeding of ecosystems with microplastics (MP)—tiny fragments less than 5 millimeters in size[1]. These diminutive particles have become ubiquitous in our environment, permeating the most remote locations and entering the food chain[2–4]. Their presence is not passive; MP interact with biological systems, leading to a growing body of research concerned with their potential health implications[5,6].

The pervasiveness of MP introduces a new variable into ecological and physiological Eqs[7,8]. These particles are not biologically inert; rather, they are active participants in the environment, potentially interacting with living organisms in myriad ways. From the depths of the oceans to the soil beneath our feet, MP have been found in various concentrations, reflecting the scale of plastic use and disposal by human societies[6,9].

MP infiltrate biological systems primarily through consumption and contact[10]. Aquatic organisms, from plankton to whales, inadvertently consume these particles, which can then ascend the food web, ultimately reaching human diets[11]. Additionally, MP are airborne, capable of traveling vast distances before being inhaled by terrestrial organisms, including humans. The skin, as the largest organ, is also a potential route of exposure through direct contact with MP-contaminated products or environments[5].

The omnipresence of MP has coincided with an increased incidence of health concerns, drawing the attention of the scientific community. Studies have reported on the physical and chemical impacts of MP on human health, including inflammatory responses and potential toxicity[6,12]. However, the long-term biological consequences, particularly in relation to aging and cellular function, are not well understood.

Aging is a complex, multifactorial process marked by a gradual decline in physiological functions. These processes interact with unprecedented complexity within and between organs, and the underlying mechanisms are still unknown. Adipose tissue crucial for energy and metabolic homeostasis, is particularly vulnerable to aging[13]. Age-associated immune responses were first identified in white adipose depots[14]. During aging, various

[1]Department of Integrated Omics for Biomedical Sciences, Graduate School, Yonsei University, Seoul 03722, Republic of Korea. [2]College of Medicine, Catholic Kwandong University, Gangneung-si 25601, Gangwon-do, South Korea. [3]Department of Convergence Science, International St. Mary's Hospital, Catholic Kwandong University, Incheon Metropolitan City 22711, South Korea. [4]The Interdisciplinary Graduate Program in Integrative Biotechnology, Yonsei University, Seoul 03722, Republic of Korea. [5]Department for Medical Science, College of Medicine, Catholic Kwandong University, Gangneung-si 25601, Republic of Korea. [6]Hanbyeol Moon and Damin Jeong contributed equally. ✉email: ksw74@cku.ac.kr

characteristic changes occur in adipose tissue, such as redistribution of adipose tissue, reduction of brown and beige fat, functional decline of adipose progenitor and stem cells, accumulation of senescent cells, and changes of immune cells[13,15]. These alterations in aging adipose tissue affect its functionality and further impact the whole body. Abnormal hormones, such as adiponectin, leptin, and resistin, have broad effects and increased proinflammatory cytokines contribute to systemic inflammation in aging adipose tissue[16–18]. Additionally, changes in aging adipose tissue can cause systematic changes through circulating miRNAs and increased ROS activity[19,20]. Accumulated oxidative stress in aging adipose tissue leads to impaired adipogenesis[21,22]. Furthermore, adipose tissue aging affects other organs infiltrated by lipids, leading to systemic inflammation, breakdown of metabolic systems, and an accelerated aging process[23]. These age-related dysfunctions in adipose tissues result in systemic negative consequences such as dyslipidemia, chronic general inflammation, insulin resistance, obesity, type 2 diabetes, and cardiovascular diseases[13,23]. Therefore, delaying the aging process of adipose tissue may be a way to prevent age-related diseases.

This research explores the connection between microplastic (MP) exposure and the aging process, specifically focusing on adipose tissue, which are central to aging and its associated systemic health outcomes. By examining how these environmental pollutants may induce cellular senescence and impair adipose tissue functions, particularly adipogenesis—the differentiation process of adipocytes—we aim to elucidate the mechanisms behind MP-induced aging. Understanding these mechanisms is essential for developing strategies to mitigate the health impacts of MPs and protect biological system integrity amid increasing environmental contamination.

Materials and methods

Animal experiments

This study involved the use of eight-week-old C57BL/6 mice, obtained from Koatech (Pyeongtaek, Korea). Upon arrival, a total of ten mice were randomly assigned into two groups, with $n=5$ mice per group. The animals were acclimatized to laboratory conditions for a period of two weeks. The acclimatization environment was strictly controlled, maintaining a temperature of 25 ± 4 °C, relative humidity at 50 ± 5%, and a 12-hour light/dark cycle to minimize stress and ensure a stable baseline for the experiments. Following the acclimatization period, the mice were subjected to oral administration of microplastic particles (MPs). The MPs were given at a concentration of 10 μg/mL, with each mouse receiving 200 μL of the suspension daily for a duration of two weeks. This exposure regime was designed to simulate a realistic scenario of microplastic ingestion in a controlled laboratory setting. Throughout the experiment, the health and behavior of the mice were closely monitored, and any signs of distress or adverse effects were recorded. Before sacrifice and tissue extraction, the mice were anesthetized with Zoletil (20 mg/kg, i.p.) and xylazine (5 mg/kg, i.p.) to minimize distress and discomfort. All experimental procedures, including animal handling, microplastic administration, euthanasia, cell culture, and data analysis, were conducted in strict accordance with the ARRIVE guidelines 2.0 and complied with all relevant institutional, national, and international guidelines regarding the ethical treatment of laboratory animals. These procedures were ethically approved by the Catholic Kwandong University School of Medicine's Committee for the Care and Use of Laboratory Animals (approval number: CKU 01-2023-007). Euthanasia was performed using CO_2 inhalation, chosen for its humane approach to minimize distress in rodents. Confirmation of death was rigorously ensured by checking for the absence of respiratory movements and reflexes immediately after exposure, verifying the effectiveness of the procedure.

Microplastic particles (MPs)

Microplastic particles used in this study were fluorescently-labeled polystyrene microplastics (PS-MPs) with a size of 1.7 ~ 2.2 μm, procured from Spherotech, Inc. (Lake Forest, IL, USA). For the in vivo experiments, these PS-MPs were suspended in phosphate-buffered saline (PBS) to a final concentration of 1.0% w/v. The suspension was stored in a dark environment to minimize any potential photodegradation of the fluorescent label, thereby preserving the fluorescence integrity of the particles. Prior to administration, the microplastic suspension was thoroughly vortexed to guarantee a homogeneous distribution of the particles, ensuring consistent dosing for each animal. This step is crucial as it affects the accuracy of the administered dose and the reliability of the subsequent findings. For the in vitro experiments involving cell cultures, the PS-MPs were similarly prepared in PBS. However, additional steps were taken to adapt the particles for cellular exposure. Human-derived stem cells (hASCs), at 70–80% confluence, were treated with PS-MPs at various concentrations (0, 1, 10 μg/ml) and incubated for 24 h in a 5% CO_2, 37 °C environment. Following this incubation period, the cells were either harvested or subjected to a differentiation process.

Senescence-associated β-Galactosidase (SA-β-gal) staining

To assess senescence in adipose tissues, SA-β-gal staining was carried out on epididymal white adipose tissue (eWAT) and inguinal white adipose tissue (iWAT) samples. These tissues were collected post-euthanasia and immediately processed for the detection of β-galactosidase activity, which is indicative of cellular senescence. The tissues were fixed to preserve cellular integrity and ensure optimal staining conditions. Following fixation, SA-β-gal staining was performed utilizing the β-Galactosidase Staining Kit (Cell Signaling Technology, Danvers, MA, USA) as per the manufacturer's instructions. This involved applying the X-gal staining solution to the tissues and incubating them at 37 °C, a temperature at which the enzyme β-galactosidase exhibits optimal activity. After adequate incubation to develop the characteristic blue color, indicative of SA-β-gal activity, tissues were washed and processed for paraffin embedding. The embedding was followed by sectioning to obtain thin slices suitable for microscopic examination.

Immunofluorescence staining

For the visualization of microplastics (MPs) within tissues and cells, immunofluorescence (IF) was performed alongside DAPI staining. Tissue samples were fixed using 4% paraformaldehyde, cryoprotected in a 30% sucrose solution for two weeks, embedded in a sucrose-gelatin medium, and frozen at -80 °C. Cryosections of 20 µm thickness were obtained and permeabilized with 0.1% Triton X-100 in PBS for 10 min. Sections were blocked with 5% bovine serum albumin (BSA) in PBS for 1 h at room temperature, then incubated overnight at 4 °C with primary antibody CD68 (1:200; Abcam, Cambridge, UK). Sections were washed with PBS and incubated with FITC-conjugated secondary antibody (1:200; EMD Millipore, Burlington, MA, USA) for 1 h at room temperature. Cells were fixed using 4% paraformaldehyde, permeabilized with 0.1% Triton X-100 in PBS for 10 min and blocked with 5% BSA in PBS for 1 h at room temperature. Cells were incubated overnight at 4 °C with primary antibody γH2A.X (1:200; Cell Signaling, Danvers, MA, USA). The following day, cells were washed with PBS and incubated with FITC-conjugated secondary antibody (1:200; EMD Millipore, Burlington, MA, USA) for 1 h at room temperature. After staining, the tissue sections and cells were rinsed to remove excess DAPI (4',6-diamidino-2-phenylindole; 1:5000 dilution, Invitrogen, Carlsbad, CA, USA) and mounted onto slides with an appropriate mounting medium (Sigma-Aldrich, St. Louis, MO, USA). The slides were examined under a confocal microscope (LSM710, Carl Zeiss, Jena, Germany), and the images were captured to identify and analyze the presence and distribution of MPs, with DAPI providing the contrast necessary to distinguish the MPs from cellular components.

Western blotting

Protein extraction from cells and tissues was performed using RIPA lysis buffer (Thermo Fisher Scientific, Waltham, MA, USA) containing both protease and phosphatase inhibitors at a concentration of 1%. The lysates were centrifuged, and the supernatant, containing the protein, was collected for further analysis. The protein concentration was quantified using an appropriate assay, and equal amounts of protein were resolved by SDS-PAGE under reducing conditions. Following electrophoresis, proteins were transferred onto PVDF membranes (EMD Millipore, Burlington, MA, USA) using a wet transfer system. To prevent nonspecific binding, membranes were blocked with 5% skim milk in Tris-buffered saline containing 0.1% Tween 20 for 1 h at room temperature. After blocking, membranes were incubated with primary antibodies specific to the target proteins overnight at 4 °C. The primary antibodies used were: MMP3, p21, LaminB1, IL6, TNF-α, c/EBPα, c/EBPβ, FABP4, PGC1α (1:1000; Santa Cruz Biotechnology, Paso Robles, CA, USA), GAPDH (1:5000; Santa Cruz Biotechnology, Paso Robles, CA, USA), HMGB1, p16, p-Histone H2A.X, p-NFκB, NFκB, PPARγ, Perilipin (1:1000; Cell Signaling, Danvers, MA, USA), CD68 (1:500; Abcam, Cambridge, UK), UCP1, Adiponectin (1:1000; Invitrogen, Carlsbad, CA, USA), and PRDM16 (1:1000; Novus Biologicals, Centennial, CO, USA). Subsequent to primary antibody binding, membranes were washed three times to remove unbound antibodies. The membranes were then incubated with horseradish peroxidase (HRP)-conjugated secondary antibodies (Santa Cruz Biotechnology, Paso Robles, CA, USA) for 1 h at room temperature. Post-secondary antibody incubation, membranes were washed and developed using enhanced chemiluminescence (ECL) detection reagents (Ab Frontier, Seoul, Korea). Protein bands were visualized using the ChemiDoc XRS + system (Bio-Rad, Hercules, CA, USA), and band intensity was quantified using image J analysis software to determine relative protein abundance.

RNA isolation and qPCR analysis

For analysis of gene expression, total RNA was isolated from cells using the TRIzol reagent (GeneAll, Seoul, South Korea), following the manufacturer's protocol for phase separation and RNA precipitation. The purity and concentration of the extracted RNA were assessed using Nanodrop (Thermo Fisher Scientific, Waltham, MA, USA). The reverse transcription was carried out using the Maxime RT PreMix kit (iNtRON Biotechnology, Seongnam, Korea), converting total RNA into complementary DNA (cDNA) according to the kit's instructions. This cDNA served as a template for subsequent polymerase chain reactions. Quantitative PCR (qPCR) was performed with SYBR Green dye on the Applied Biosystems StepOnePlus real-time PCR system (Foster City, CA, USA) to amplify and quantify the expression of target genes. The housekeeping gene GAPDH was used as an endogenous control to normalize the expression levels of the target genes. Relative quantification of gene expression was determined using the $2^{\Delta\Delta Ct}$ method, which calculates the fold change in expression of the target gene relative to the control. Primer sequences are listed in an accompanying Table 1.

Cell culture and adipocyte differentiation

Human adipose-derived stem cells (hASCs) were obtained from Lonza (Walkersville, MD, USA) and cultured in low-glucose Dulbecco's Modified Eagle's Medium (DMEM, Gibco, Waltham, MA, USA). The culture medium was supplemented with 5.56 mM glucose, 4 mM L-glutamine, and 1 mM sodium pyruvate, and 10% fetal bovin serum (FBS, Gibco Waltham, MA, USA) to support cell growth and maintenance. For adipogenic differentiation, hASCs were exposed to an induction cocktail containing 5 µg/mL insulin (Sigma-Aldrich, St. Louis, MO, USA), 2 µg/mL dexamethasone (Dexa, Sigma-Aldrich, St. Louis, MO, USA), and 0.5 mM 3-isobutyl-1-methylxanthine (IBMX, Sigma-Aldrich, St. Louis, MO, USA) in DMEM/F-12 medium for 3 days to initiate adipogenic commitment. Subsequent to induction, the differentiation medium for brown adipocytes (BACs) was supplemented with 1 nM triiodothyronine (T3), 0.5 µM rosiglitazone and 125 µM indomethacin to promote brown fat phenotype characteristics over a period of 6 days. In contrast, white adipocytes (WACs) were further matured in F-12 medium enhanced with 10 µg/mL insulin to encourage the development of white fat cell features.

Oil red O (ORO) staining

To evaluate adipocyte differentiation, Oil Red O (ORO) staining was performed. Human adipose-derived stem cells (hASCs) and differentiated adipocytes were fixed with 4% formaldehyde for 30 min to preserve cell

Species	Genes		Primer sequence (5' – 3')
Human	*MMP3*	F [a)]	CACTCACAGACCTGACTCGGTT
		R [b)]	AAGCAGGATCACAGTTGGCTGG
	HMGB1	F	GCGAAGAAACTGGGAGAGATGTG
		R	GCATCAGGCTTTCCTTTAGCTCG
	CDKN1A	F	CTCGTGCTGATGCTACTGAGGA
		R	GGTCGGCGCAGTTGGGCTCC
	CDKN2A	F	AGGTGGACCTGGAGACTCTCAG
		R	TCCTCTTGGAGAAGATCAGCCG
	TERT	F	GCCGATTGTGAACATGGACTACG
		R	GCTCGTAGTTGAGCACGCTGAA
	LMNB1	F	ATGAGGACCAGGTGGAGCAGTA
		R	ACCAGGTTGCTGTTCCTCTCAG
	H2AFX	F	CGGCAGTGCTGGAGTACCTCA
		R	AGCTCCTCGTCGTTGCGGATG
	IL6	F	TCAATATTAGAGTCTCAACCCCCA
		R	GTTCATAGCTGGGCTCCTGG
	TNF	F	CACCACTTCGAAACCTGGGA
		R	TGTAGGCCCCAGTGAGTTCT
	PRDM16	F	TGGTTGCCTGCATGAGTGTG
		R	CGGTTAGGAAGACAGCCGAA
	PPARG	F	GCAAACCCCTATTCCATGCTG
		R	ACGGAGCTGATCCCAAAGTT
	UCP1	F	GTGTCGGCTCTTATCGCTGG
		R	CCAAGTCGCAAGAAGGAAGG
	CEBPB	F	CGACGAGTACAACCGGC
		R	TGCTTGAACAAGTTCCGCAG
	ADIPOQ	F	CAGGCCGTGATGGCAGAGATG
		R	GGTTTCACCGATGTCTCCCTTAG
	PPARGC1A	F	TGACCCCGTCTCTCTGAAGT
		R	CTCAGAGTCCTGGTTGCACAT
	GAPDH	F	CATGGGTGTGAACCATGAGA
		R	GGTCATGAGTCCTTCCACGA
Mouse	*Mmp3*	F	TTTAAAGGAAATCAGTTCTGGGCTATA
		R	CGATCTTCTTCACGGTTGCA
	Hmgb1	F	CCAAGAAGTGCTCAGAGAGGTG
		R	GTCCTTGAACTTCTTTTTGGTCTC
	Cdkn1a	F	ACTACCAGCTGTGGGGTGAG
		R	TCGGACATCACCAGGATTGG
	Cdkn12a	F	CGAACTCGAGGAGAGCCATC
		R	GGGGTACGACCGAAAGAGTT
	H2afx	F	AACGACGAGGAGCTCAACAAGC
		R	TGGCGCTGCTCTTCTTGGGCA
	Tert	F	GAAAGTAGAGGATTGCCACTGGC
		R	CGTATGTGTCCATCAGCCAGAAC
	Lmnb1	F	AGGAAGAGCTGGAGCAGACCTA
		R	GCAGGTTAGAGAGCTGTGAGGA
	IL6	F	TACCACTTCACAAGTCGGAGGC
		R	CTGCAAGTGCATCATCGTTGTTC
	Tnf	F	GCCACCACGCTCTTCTGTCT
		R	GGTCTGGGCCATAGAACTGATG
	Cd68	F	AGCTGCCTGACAAGGGACAC
		R	TGAGAGGCAGCAAGAGGGA
	GAPDH	F	CATCACTGCCACCCAGAAGACTG
		R	ATGCCAGTGAGCTTCCCGTTCAG

Table 1. Sequences of primers used for qRT-PCR. (a) F, sequence from sense strands; (b) R, sequence from anti-sense strands

morphology and facilitate lipid staining. After fixation, cells were washed thrice with distilled water to remove any residual fixative. The cells were then prepared for staining by rinsing with 60% isopropanol, which helps in the penetration of the ORO dye into the lipid droplets. Subsequently, the cells were incubated with the ORO solution (Sigma, St. Louis, MO, USA) for 30 min at room temperature, allowing the stain to selectively color the neutral triglycerides and lipids within the cells. Following the incubation period, the excess stain was washed away with distilled water to reduce background staining and enhance contrast. The stained adipocytes were then examined under an optical microscope. To quantitatively evaluate the lipid accumulation in the stained adipocytes, the Oil Red O (ORO) stain was eluted using 100% Propylene glycol (DUKSAN, Ansan, Korea). The stained cells were incubated with 100% Propylene glycol for 30 min at room temperature. After the incubation period, the absorbance of the eluted dye was measured at 450 nm using a spectrophotometer. This absorbance value correlates with the amount of lipid content in the cells, providing a quantitative measure of adipocyte differentiation.

Statistical analysis

All data were analyzed using one-way analysis of variance (ANOVA) with the Statistical Package for the Social Sciences (SPSS, version 14.0 K). Results are presented as mean ± SEM. Significant differences between group means were determined using the protected least-significant difference (LSD) test at $p < 0.05$.

Results

MPs induce senescence of eWAT and iWAT

This study was designed to investigate the accumulation of microplastics (MPs) and its potential impact on tissue aging in epididymal white adipose tissue (eWAT) and inguinal white adipose tissue (iWAT) (Fig. 1A). The experiment confirmed that, following 14 days of oral administration, MPs were clearly visible as distinct fluorescent dots in both eWAT and iWAT (Fig. 1B). We observed no significant differences in the weights of eWAT and iWAT between the control and MP-treated groups. However, adipocyte size was slightly reduced in the MP-treated eWAT group compared to the control, while no significant changes were noted in iWAT (Fig. 2A). An increase in SA-β-gal activity, a key indicator of cellular senescence, was observed in both eWAT and iWAT due to the accumulation of MPs, as shown in Fig. 2B. This suggests that the presence of MPs induced an aging response. Senescence signaling pathways were further investigated by examining specific senescence markers, including MMP3, a marker associated with extracellular matrix remodeling; HMGB1, known for its role in inflammation; p21, p16, both associated with cell cycle arrest; p-Histone H2A.X, a marker of DNA damage and LaminB1, which is associated with nuclear structure and stability and is known to decrease in senescent cells[24,25]. The results of Western blot and real-time qPCR analyses indicate an upregulation of senescence markers in the MPs groups (Fig. 2C, D). This observation revealed the upregulation of senescence signaling pathways induced by MPs. Taken together, these finding demonstrate that MPs induce aging in eWAT and iWAT through the upregulation of SA-β-gal activity, as well as senescence marker.

MPs amplify inflammation and aging in eWAT and iWAT

As revealed in previous studies, aging and inflammation are known to engage in an intricate interplay[19]. Developing this understanding, we confirmed an association between inflammation and aging in response to MPs exposure. Through Western blot examinations, increased levels of key inflammatory markers such as NF-kB, IL6, TNF-a, and CD68 were observed (Fig. 3A). These markers play crucial roles in the inflammatory response, with IL6 and TNF-a particularly associated with the senescence-associated secretory phenotype (SASP)[26,27]. CD68, a macrophage marker, signifies an increase in macrophage infiltration within adipose tissues, indicating increased macrophage[28,29]. These results demonstrated the upregulation of inflammatory markers at the molecular level, providing comprehensive evidence of the interconnected relationship between inflammation and aging induced by MPs. Notably, the presence of CD68 was visually confirmed through fluorescent staining, adding a compelling visual dimension to the inflammatory impact of MPs and confirming their potential role in the aging cascade within adipose tissues (Fig. 3B, C). In conclusion, these findings provide robust evidence of the connected relationship between inflammation and aging induced by MPs, identifying on the intricate mechanisms at play within adipose tissues.

MPs internalization and induce senescence in hASCs

After confirming the accumulation of MPs in eWAT and iWAT, we proceeded to investigate the internalization of MPs within adipocytes. To investigate this, we subjected human adipose-derived stem cells (hASCs) to different concentrations (0ug/ml, 1ug/ml, and 10ug/ml) for a duration of 24 h. Subsequent experiments demonstrated the internalization of MPs into hASCs (Fig. 4A). To investigate whether MPs induce senescence in hASCs, we treated with different concentrations of MPs and performed SA-β-gal staining. The results revealed an increase in SA-β-gal positive cells with MPs groups (Fig. 4B). H2AX staining (Fig. 4C) also showed an increase in positive cells with higher MP concentrations. Western blot analysis further confirmed the upregulation of both senescence and inflammatory markers, considering the known relationship between cell senescence and inflammation as revealed in the previous study. (Fig. 4D). Western blot results indicated an elevation in inflammatory markers with increasing MP concentrations (Fig. 4D). The reduced presence of lipid droplets in differentiated cells may offer reasons for these differentiation disturbances[30,31]. This observation suggests potential disruptions in the differentiation process induced by MPs exposure. Furthermore, cells differentiated from hASCs into WACs and BACs exhibited an increase in senescence markers dependent on MP concentration, as shown in Fig. 5. Notably, the internalization of MPs was not restricted to hASCs alone; cells differentiated from hASCs into white adipocytes (WAC) or brown adipocytes (BAC) also exhibited the presence of MPs (Fig. 5A). The results of Western blot and real-time qPCR analyses indicate an upregulation of senescence markers dependent on

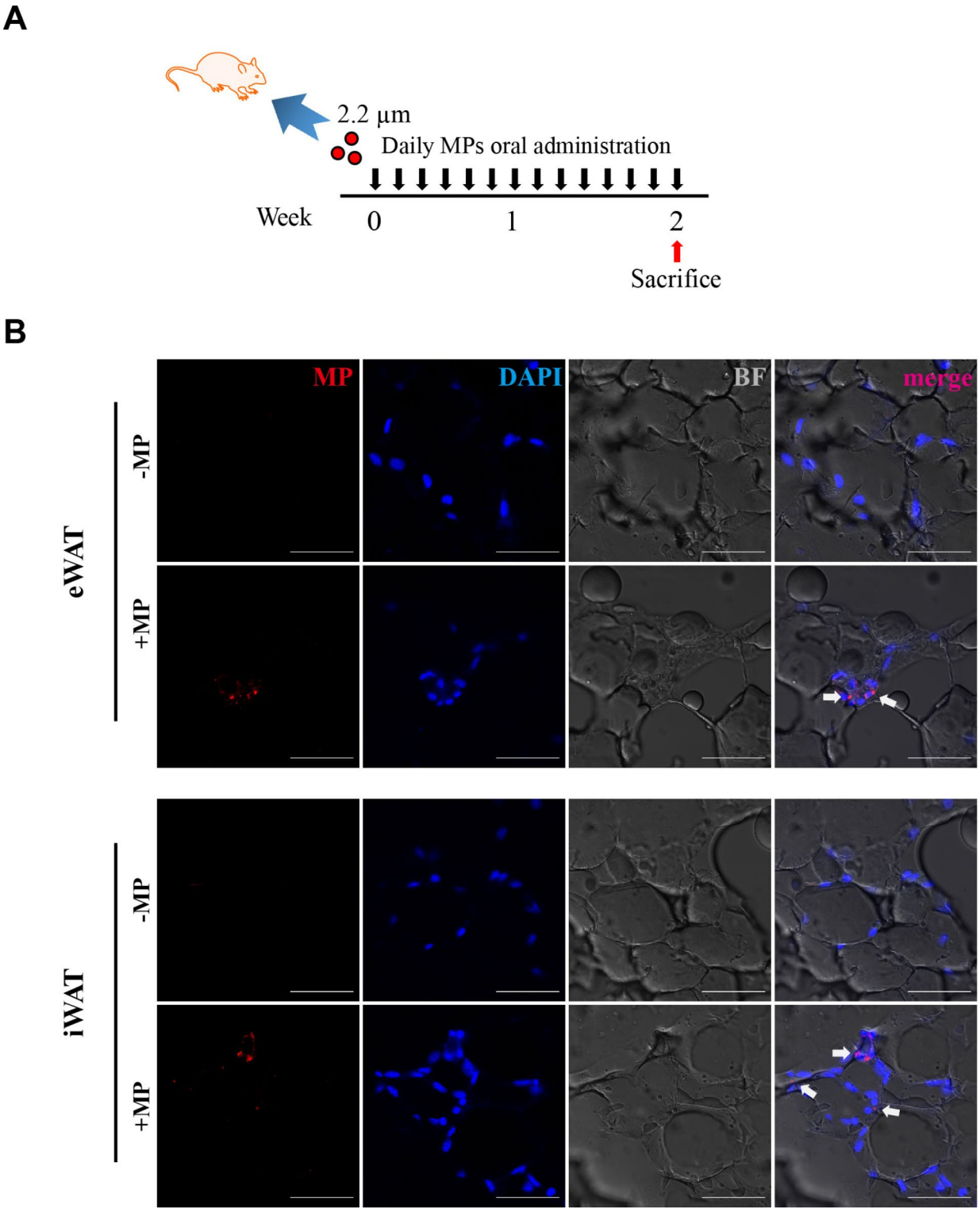

Fig. 1. Microplastics (MPs) accumulation in epididymal (eWAT) and inguinal (iWAT) white adipose tissue following oral administration in mice. (**a**) Schematic diagram illustrating the experimental timeline for oral administration of MPs in mice. (**b**) Histological sections of eWAT and iWAT from mice treated with MPs for 2 weeks, visualized under a microscope. The sections are stained with nuclei (DAPI, blue), MPs (Rhodamine, red), and brightfield (BF, gray). Scale bars represent 50 μm.

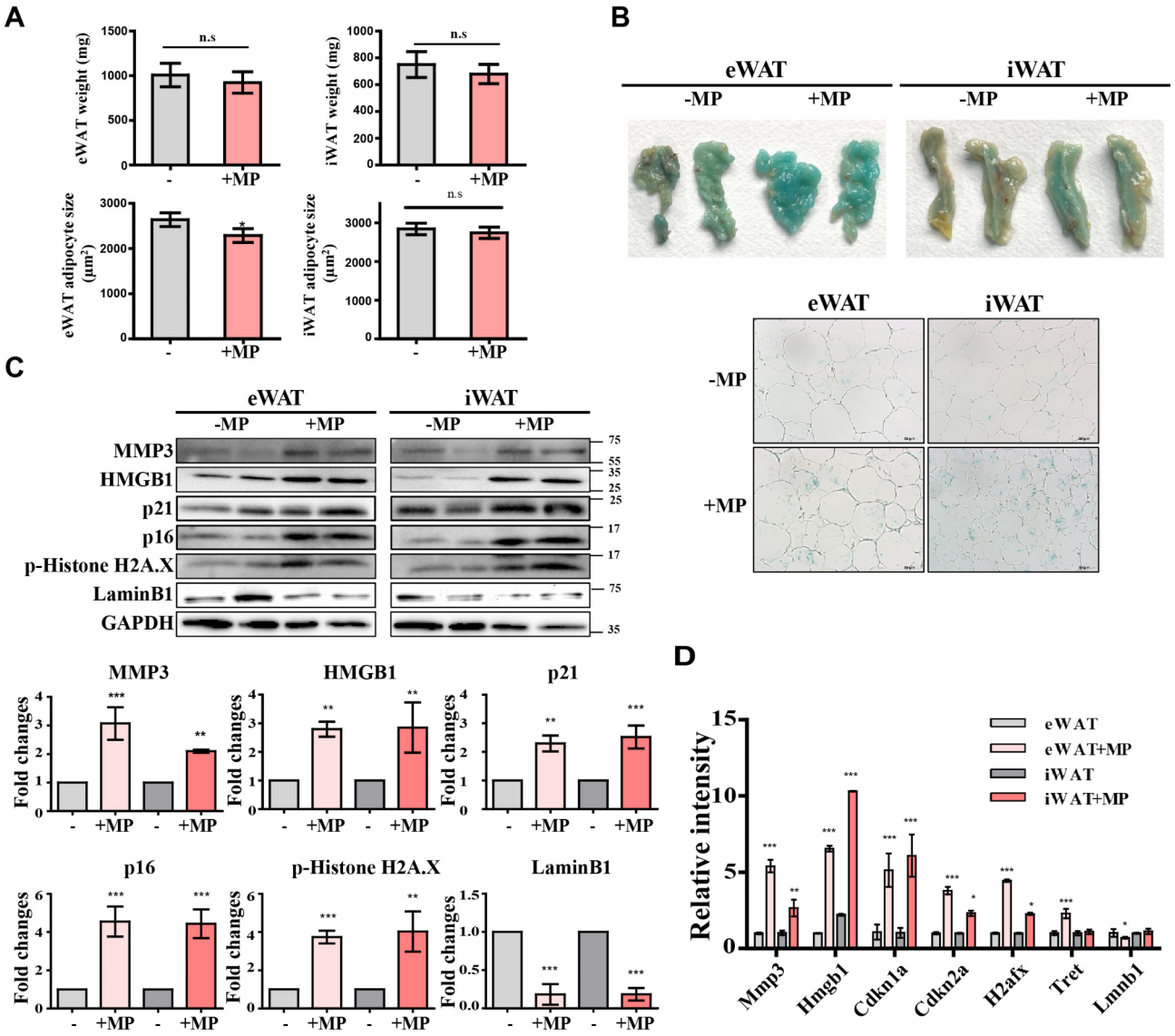

Fig. 2. Senescence and protein expression analysis in adipose tissue post-MPs exposure. (**a**) eWAT and iWAT weight and adipocyte size in control and MP-treated groups. (**b**) X-gal staining depicting senescent cells in section of adipose tissue after MPs treatment. Scale bars represent 50 μm. (**c**) Representative western blot images showing protein expression in eWAT and iWAT ($n=3$) treated with either PBS or MPs for 2 weeks. Original blots/uncropped images are presented in Supplementary Figures. (**d**) qPCR results of eWAT and iWAT ($n=3$) tissues under the same treatment conditions. Statistical significance is denoted as $^{*}p<0.05$, $^{**}p<0.01$, and $^{***}p<0.001$ compared to the control group.

MP concentration, indicating that MPs induce senescence signaling pathways (Fig. 5B, C). Additionally, the concurrent elevation in inflammatory markers underscores the multifaceted impact of MPs on both senescence and inflammation in hASC-derived cells. Notably, MPs not only induced senescence in hASCs but also triggered aging in their differentiated forms, WACs and BACs.

MPs impair adipocyte differentiation in hASCs

Previous results suggest that senescence in hASCs may diminish their differentiation capacity, potentially leading to adipocyte dysfunction. Adipocyte differentiation involves the formation and growth of lipid droplets (LDs), which are cellular structures essential for lipid storage and transport within adipose tissue. To assess the impact of MPs on hASC differentiation, we performed Oil Red O (ORO) staining on WACs and BACs—adipocytes differentiated from MPs-treated hASCs. The results showed a decrease in lipid droplet biogenesis, indicating impaired adipocyte differentiation (Fig. 6A). Quantitative analysis of ORO staining revealed that the optical density (OD) values decreased with increasing MP concentrations, further confirming the negative impact of MPs on adipocyte differentiation. Furthermore, Western blot analyses and real-time qPCR of WACs and BACs revealed a reduction in the levels of pro-adipogenic markers, including PPARγ, C/EBPα, and Adiponectin, as

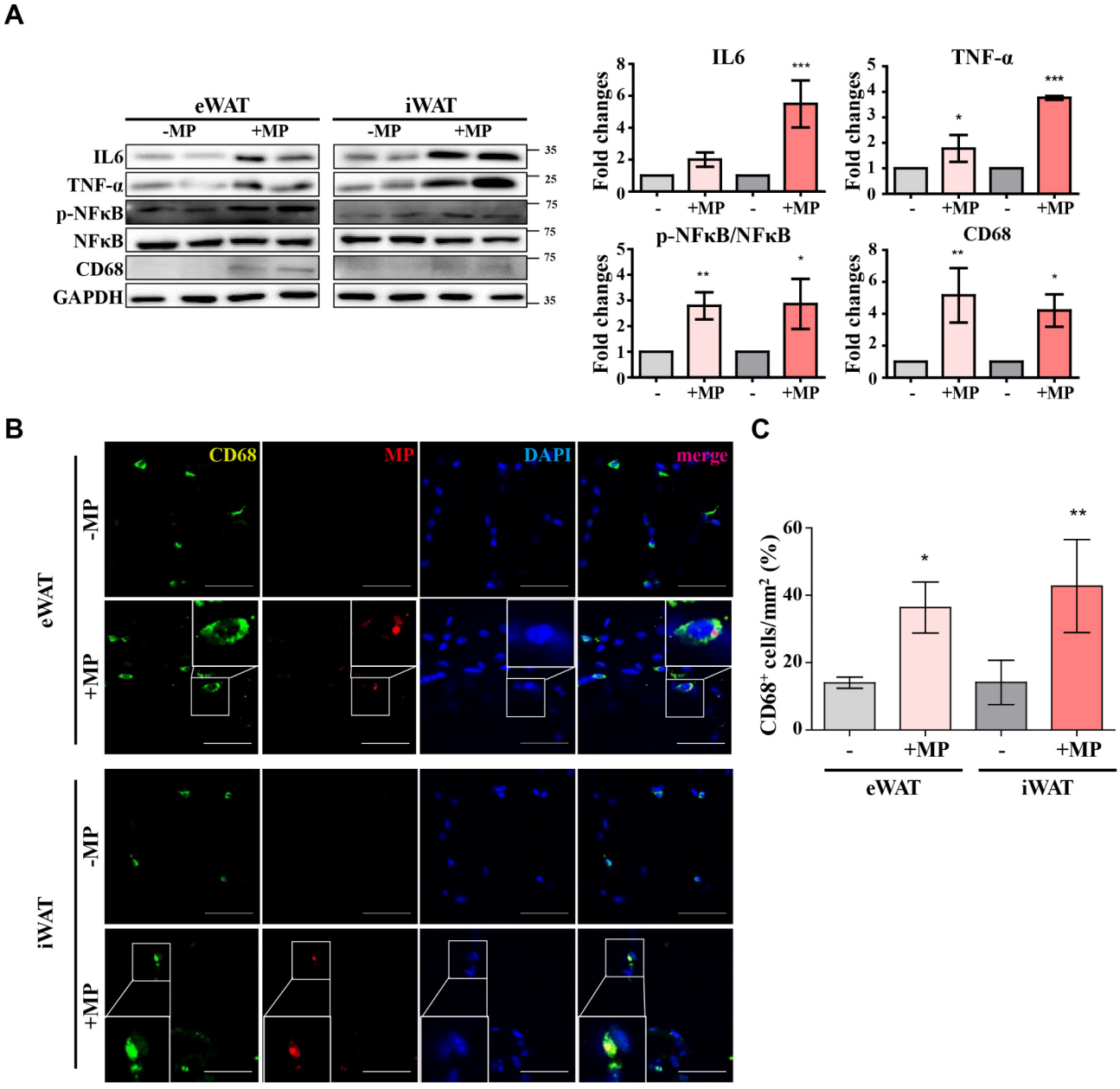

Fig. 3. Increased inflammatory marker in adipose tissue upon MPs exposure. (**a**) Western blot analysis illustrating the expression of inflammation markers CD68, NF-kB, TNF-α, and IL-6. Original blots/uncropped images are presented in Supplementary Figures. (**b**) Confocal microscopy images showing CD68 staining (FITC, green), indicative of macrophage presence within adipose tissue, MPs (Rhodamine, red), and nuclei (DAPI, blue). Scale bar = 50 µm. ($n = 3$) (**c**) Quantification of the number of CD68-positive cells. ($n = 3$) Significance levels are indicated as $^{*}p < 0.05$, $^{**}p < 0.01$, and $^{***}p < 0.001$ relative to the control.

MP concentration increased (Fig. 6B, C). While some markers showed slight increases at lower concentrations of MPs, a significant reduction was observed at higher concentrations. These findings underscore the inhibitory effect of MPs on adipocyte differentiation.

Discussion

This study provides comprehensive insights into the impact of microplastic particles (MPs) on adipose tissue aging and dysfunction, focusing on both in vivo (epididymal and inguinal white adipose tissue - eWAT and iWAT) and in vitro (human adipose-derived stem cells - hASCs) models. We administered 1.7 ~ 2.2 µm polystyrene microplastics (PS-MPs) orally to mice, observing their accumulation in eWAT and iWAT. This accumulation correlated with increased aging markers, including SA-β-gal activity and senescence markers MMP3, HMGB1, p21, p16, and phosphorylated Histone H2A.X[24,25].

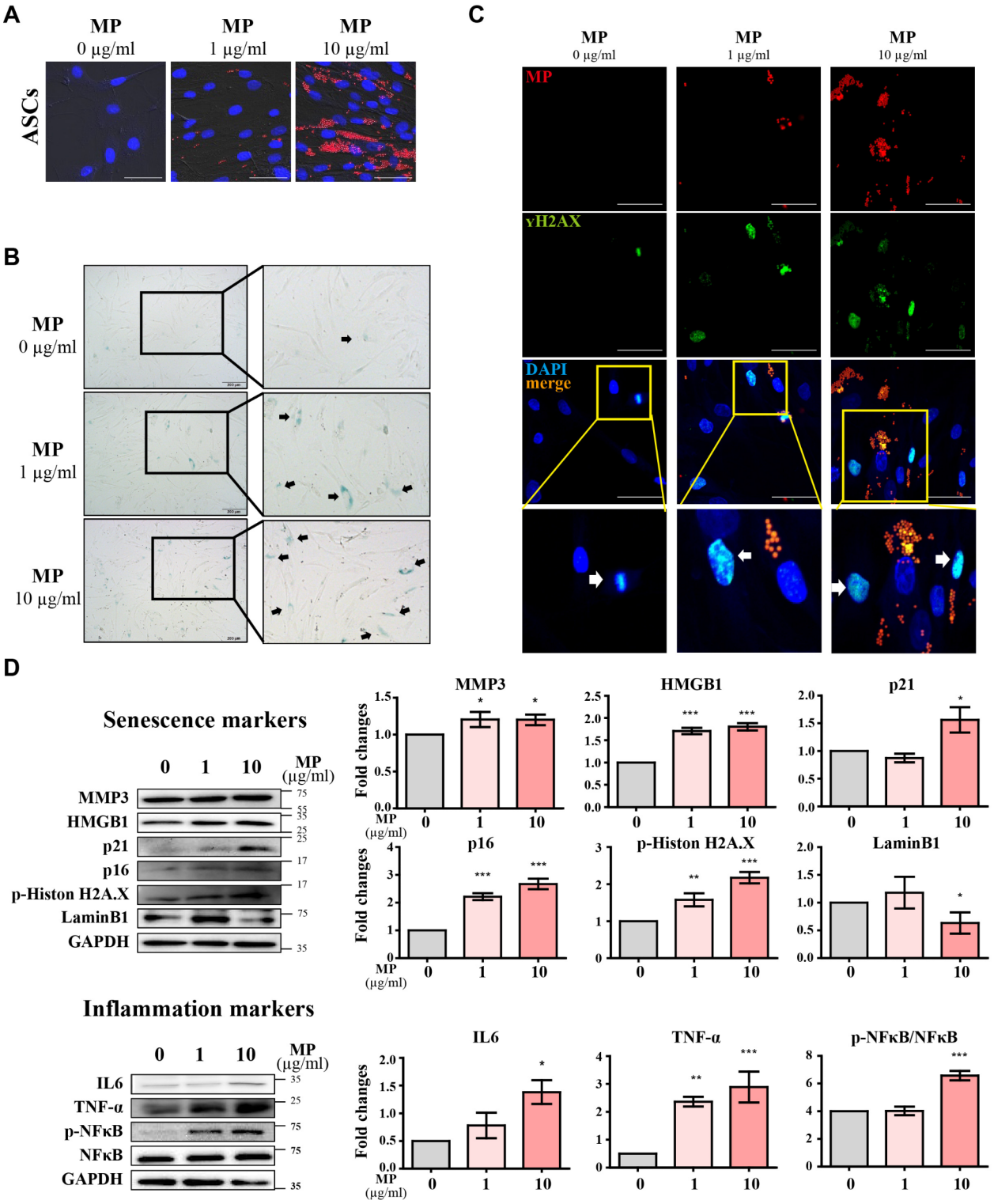

Fig. 4. Induction of senescence in human adipose-derived stem cells (hASCs) by MPs Exposure. (**a**) Fluorescence microscopy images showing the internalization of MPs in hASCs. The sections are stained with MPs (Rhodamine, red) and nuclei (DAPI, blue). Scale bar = 50 μm. (**b**) Detection of senescent cells in hASCs MPs treatment, indicated by X-gal positive staining. Scale bar = 100 μm. (**c**) Fluorescence images showing the expression of γH2AX in hASCs treated with MPs. The sections are stained with MPs (Rhodamine, red), γH2AX (FITC, green), and nuclei (DAPI, blue). Scale bar = 100 μm. (**d**) Western blot images of senescence and inflammation markers in hASCs treated with MPs for 24 h. Original blots/uncropped images are presented in Supplementary Figures. Data are presented as mean ± SEM ($n = 3$ per group), with significance indicated as $^{*}p < 0.05$, $^{**}p < 0.01$, and $^{***}p < 0.001$ compared to control.

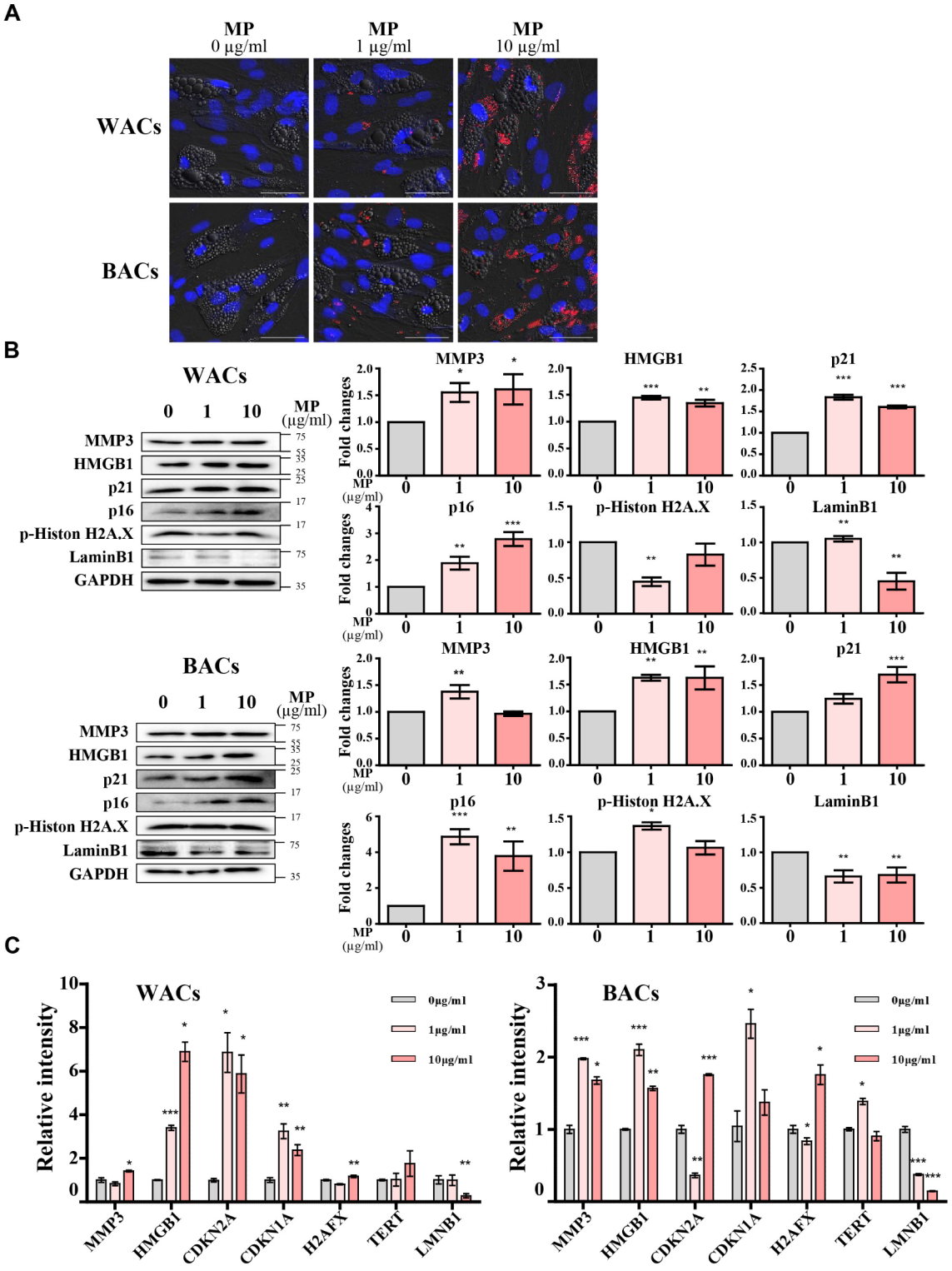

Fig. 5. Effect of MPs on senescence markers in cells differentiated from hASCs into WACs and BACs. (**a**) Fluorescence microscopy images showing the internalization of MPs in WACs and BACs (**b**) Western blot showing the expression of senescence markers in WACs and BACs following MP treatment. Original blots/uncropped images are presented in Supplementary Figures. (**c**) qPCR confirmation of upregulated senescence-associated genes in WACs and BACs following MP treatment confirmed by. Data are presented as mean ± SEM ($n = 3$ per group), with significance indicated as $^{*}p < 0.05$, $^{**}p < 0.01$, and $^{***}p < 0.001$ compared to the control.

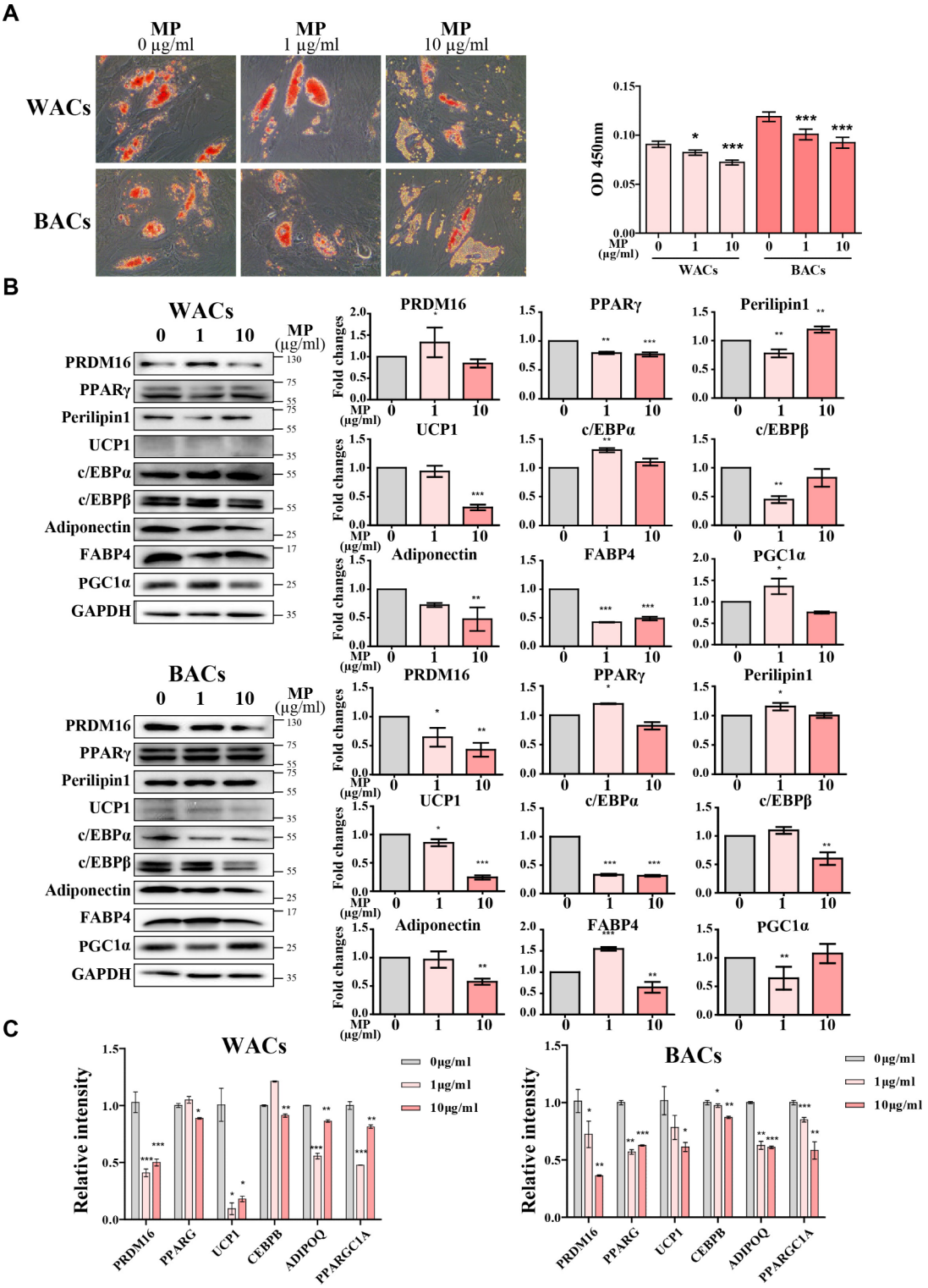

Fig. 6. Impact of MPs exposure on adipogenic differentiation in hASCs. (**a**) Oil Red O (ORO) staining on WACs and BACs—adipocytes differentiated from MPs-treated hASCs. The ORO-stained cells were visualized under a microscope, and the extracted ORO was quantified to assess lipid accumulation. (**b**) Western blot analysis of adipogenic markers in WACs and BACs derived from hASCs treated with MPs for 24 h. Original blots/uncropped images are presented in Supplementary Figures. (**c**) Quantification of transcript expression levels of adipogenic markers, normalized to GAPDH. Data are mean ± SEM ($n = 3$ per group), with statistical significance marked as $^{*}p < 0.05$, $^{**}p < 0.01$, and $^{***}p < 0.001$ compared to the control.

In vitro experiments showed that MPs were internalized by undifferentiated hASCs and remained within the cells during their differentiation process, demonstrating the general susceptibility of adipose cells to MPs. This exposure led to increased SA-β-gal activity and further upregulation of senescence markers, aligning with previous research identifying MPs as environmental stressors that induce oxidative stress and DNA damage, contributing to cellular aging[32,33].

Our findings suggest that MP exposure does not significantly affect the weight of eWAT or iWAT. However, the slight reduction in adipocyte size in MP-treated eWAT may indicate a specific impact of MPs on adipocyte morphology. The observed adipocyte sizes were larger than commonly reported values, underscoring the need for further research to fully understand these effects. Both in vivo and in vitro exposures to MPs also increased inflammatory markers such as NF-kB, IL6, TNF-α, and CD68[34,35]. The concurrent rise in these markers with MP concentrations links microplastic exposure to cellular senescence and inflammation. The study confirms that inflammation both contributes to and results from cellular aging. Cells in senescence exhibit changes in their secretome, known as the senescence-associated secretory phenotype (SASP), which involves upregulating pro-inflammatory cytokines, further fueling inflammation[36,37]. This study builds on existing research that characterizes MPs as xenobiotics that activate pro-inflammatory cytokines, primarily secreted by immune cells. Moreover, inflammation itself, regardless of MP exposure, is a known factor that contributes to cellular aging. Chronic inflammation, often referred to as "inflammaging," accelerates the aging process by promoting cellular damage and senescence. Pro-inflammatory cytokines, such as IL6 and TNF-α, play a critical role in this process, exacerbating cellular stress and dysfunction[38,39].

We further connect microplastic exposure with cellular senescence, highlighting how inflammation is crucial in both initiating and maintaining cellular aging while cellular senescence can also stimulate inflammatory responses. The dramatic changes in the secretomes of senescent cells, characteristic of SASP, involve the release of multiple pro-inflammatory cytokines[37,40]. Our results, indicating an increase in inflammatory markers such as IL6 and TNF-α associated with SASP in adipose cells, underline the dual role of MPs in inducing cellular senescence and inflammation. These findings are significant, considering the implications of inflammation and dysfunction from aging adipose tissue in metabolic dysregulation and the onset of age-related diseases.

The presence of microplastic particles (MPs) disrupted normal adipogenic differentiation, evidenced by reduced lipid droplet formation and decreased expression of adipogenic markers in differentiated white and brown adipose cells (WACs and BACs). While our findings suggest that MPs may interfere with adipogenesis by affecting the differentiation of preadipocytes into mature adipocytes, the precise mechanisms—whether through inhibition of lipid droplet biogenesis, promotion of lipolysis, or another pathway—remain unclear and warrant further investigation. Additionally, the decreased levels of key functional markers such as PRDM16 and UCP1, which regulate adaptive thermogenesis and adipogenesis in BACs, further indicate dysfunction. This aligns with studies showing a correlation between impaired adipogenesis and the increased release of TNF-α and other SASP-associated inflammatory markers in aging adipose tissue.

Our findings raise significant concerns about the potential health impacts of MPs exposure, particularly in relation to adipose tissue health and metabolic function. The study highlights the need for further research to understand the long-term consequences of MPs accumulation in biological systems and the mechanisms underlying their impact on cellular aging and inflammation. The results also underscore the importance of addressing environmental microplastic pollution as a public health issue, given its widespread presence and the growing evidence of its biological impacts.

Conclusions

In conclusion, this study elucidates the multifaceted impact of microplastic exposure on adipose tissue, demonstrating its role in inducing cellular senescence, amplifying inflammatory responses, and impairing differentiation capacity. These findings contribute to a deeper understanding of the potential adverse effects of environmental contaminants on biological aging and tissue function, offering a foundation for future research and public health initiatives aimed at mitigating these effects.

Data availability

Data is provided within the manuscript or supplementary information files.

Received: 20 May 2024; Accepted: 30 September 2024
Published online: 13 October 2024

References

1. Bostan, N. *et al.* Toxicity assessment of microplastic (MPs); a threat to the ecosystem. *Environ. Res.* **234**, 116523. https://doi.org/10.1016/j.envres.2023.116523 (2023).
2. Cverenkarova, K., Valachovicova, M., Mackulak, T., Zemlicka, L. & Birosova, L. Microplastics in the Food Chain. *Life* **11**. https://doi.org/10.3390/life11121349 (2021).
3. Lehel, J. & Murphy, S. Microplastics in the Food Chain: Food Safety and Environmental aspects. *Rev. Environ. Contam. Toxicol.* **259**, 1–49. https://doi.org/10.1007/398_2021_77 (2021).
4. van Raamsdonk, L. W. D. *et al.* Current Insights into Monitoring, Bioaccumulation, and Potential Health Effects of Microplastics Present in the Food Chain. *Foods* **9**, (2020). https://doi.org/10.3390/foods9010072
5. Barcelo, D., Pico, Y., Alfarhan, A. H. & Microplastics Detection in human samples, cell line studies, and health impacts. *Environ. Toxicol. Pharmacol.* **101**, 104204. https://doi.org/10.1016/j.etap.2023.104204 (2023).
6. Marfella, R. *et al.* Microplastics and nanoplastics in Atheromas and Cardiovascular events. *N. Engl. J. Med.* **390**, 900–910. https://doi.org/10.1056/NEJMoa2309822 (2024).
7. Winiarska, E., Jutel, M. & Zemelka-Wiacek, M. The potential impact of nano- and microplastics on human health: understanding human health risks. *Environ. Res.* **251**, 118535. https://doi.org/10.1016/j.envres.2024.118535 (2024).

8. Zhang, Q. *et al*. Recent advances in toxicological research and potential health impact of microplastics and nanoplastics in vivo. *Environ. Sci. Pollut. Res. Int.* **29**, 40415–40448. https://doi.org/10.1007/s11356-022-19745-3 (2022).
9. Guo, J. J. *et al*. Source, migration and toxicology of microplastics in soil. *Environ. Int.* **137**, 105263. https://doi.org/10.1016/j.envint.2019.105263 (2020).
10. Mohamed Nor, N. H., Kooi, M., Diepens, N. J. & Koelmans, A. A. Lifetime Accumulation of Microplastic in children and adults. *Environ. Sci. Technol.* **55**, 5084–5096. https://doi.org/10.1021/acs.est.0c07384 (2021).
11. Zhang, Q. *et al*. A review of Microplastics in Table Salt, drinking Water, and air: direct human exposure. *Environ. Sci. Technol.* **54**, 3740–3751. https://doi.org/10.1021/acs.est.9b04535 (2020).
12. Editorial to accompany the Minderoo-Monaco Commission on, P., Human Health in the journal, A. o. G. H. & & Neira, M. The Minderoo-Monaco Commission on Plastics and Human Health. *Ann. Glob. Health* **89**, 22. https://doi.org/10.5334/aogh.4083 (2023).
13. Ou, M. Y., Zhang, H., Tan, P. C., Zhou, S. B. & Li, Q. F. Adipose tissue aging: mechanisms and therapeutic implications. *Cell Death Dis.* **13**, 300. https://doi.org/10.1038/s41419-022-04752-6 (2022).
14. Schaum, N. et al. Ageing hallmarks exhibit organ-specific temporal signatures. *Nature* **583**, 596–602. https://doi.org/10.1038/s41586-020-2499-y (2020).
15. Kuk, J. L., Saunders, T. J., Davidson, L. E. & Ross, R. Age-related changes in total and regional fat distribution. *Ageing Res. Rev.* **8**, 339–348. https://doi.org/10.1016/j.arr.2009.06.001 (2009).
16. Scarpace, P. J., Matheny, M., Moore, R. L. & Tumer, N. Impaired leptin responsiveness in aged rats. *Diabetes*. **49**, 431–435. https://doi.org/10.2337/diabetes.49.3.431 (2000).
17. Antuna-Puente, B., Feve, B., Fellahi, S. & Bastard, J. P. Adipokines: the missing link between insulin resistance and obesity. *Diabetes Metab.* **34**, 2–11. https://doi.org/10.1016/j.diabet.2007.09.004 (2008).
18. Starr, M. E., Evers, B. M. & Saito, H. Age-associated increase in cytokine production during systemic inflammation: adipose tissue as a major source of IL-6. *J. Gerontol. A*. **64**, 723–730. https://doi.org/10.1093/gerona/glp046 (2009).
19. Thomou, T. *et al*. Adipose-derived circulating miRNAs regulate gene expression in other tissues. *Nature* **542**, 450–455. https://doi.org/10.1038/nature21365 (2017).
20. Furukawa, S. *et al*. Increased oxidative stress in obesity and its impact on metabolic syndrome. *J. Clin. Investig.* **114**, 1752–1761. https://doi.org/10.1172/JCI21625 (2004).
21. Findeisen, H. M. *et al*. Oxidative stress accumulates in adipose tissue during aging and inhibits adipogenesis. *PloS ONE* **6**, e18532. https://doi.org/10.1371/journal.pone.0018532 (2011).
22. Finkel, T. & Holbrook, N. J. Oxidants, oxidative stress and the biology of ageing. *Nature* **408**, 239–247. https://doi.org/10.1038/35041687 (2000).
23. DeNino, W. F. *et al*. Contribution of abdominal adiposity to age-related differences in insulin sensitivity and plasma lipids in healthy nonobese women. *Diabetes Care* **24**, 925–932. https://doi.org/10.2337/diacare.24.5.925 (2001).
24. Wang, A. S. & Dreesen, O. Biomarkers of Cellular Senescence and skin aging. *Front. Genet.* **9**. https://doi.org/10.3389/fgene.2018.00247 (2018).
25. Baker, D. J. & Petersen, R. C. Cellular senescence in brain aging and neurodegenerative diseases: evidence and perspectives. *J. Clin. Investig.* **128**, 1208–1216. https://doi.org/10.1172/JCI95145 (2018).
26. Li, X. *et al*. Inflammation and aging: signaling pathways and intervention therapies. *Signal. Transduct. Target. Ther.* **8**. https://doi.org/10.1038/s41392-023-01502-8 (2023).
27. Coppe, J. P., Desprez, P. Y., Krtolica, A. & Campisi, J. The senescence-associated secretory phenotype: the dark side of tumor suppression. *Annu. Rev. Pathol.* **5**, 99–118. https://doi.org/10.1146/annurev-pathol-121808-102144 (2010).
28. Gollisch, K. S. *et al*. Effects of exercise training on subcutaneous and visceral adipose tissue in normal- and high-fat diet-fed rats. *Am. J. Physiol. Endocrinol. Metab.* **297**, E495–504. https://doi.org/10.1152/ajpendo.90424.2008 (2009).
29. Di Gregorio, G. B. *et al*. Expression of CD68 and macrophage chemoattractant protein-1 genes in human adipose and muscle tissues: association with cytokine expression, insulin resistance, and reduction by pioglitazone. *Diabetes* **54**, 2305–2313. https://doi.org/10.2337/diabetes.54.8.2305 (2005).
30. Ploner, C. *et al*. Oxidant therapy improves adipogenic differentiation of adipose-derived stem cells in human wound healing. *Stem Cell Res. Ther.* **12**. https://doi.org/10.1186/s13287-021-02336-3 (2021).
31. Perumal, N. L. *et al*. Suppression of lipid Accumulation in the differentiation of 3T3-L1 preadipocytes and human adipose stem cells into adipocytes by TAK-715, a specific inhibitor of p38 MAPK. *Life* **13**. https://doi.org/10.3390/life13020412 (2023).
32. Wu, D., Zhang, M., Bao, T. T. & Lan, H. Long-term exposure to polystyrene microplastics triggers premature testicular aging. *Part. Fibre Toxicol.* **20**. https://doi.org/10.1186/s12989-023-00546-6 (2023).
33. Kannan, K. & Vimalkumar, K. A. Review of human exposure to Microplastics and insights into Microplastics as Obesogens. *Front. Endocrinol.* **12**, 724989. https://doi.org/10.3389/fendo.2021.724989 (2021).
34. Anilkumar, S. & Wright-Jin, E. NF-kappaB as an Inducible Regulator of Inflammation in the Central Nervous System. *Cells* **13**. https://doi.org/10.3390/cells13060485 (2024).
35. Pulvirenti, E. *et al*. Effects of Nano and Microplastics on the inflammatory process: in Vitro and in vivo studies systematic review. *Front. Biosci.* **27**. https://doi.org/10.31083/j.fbl2710287 (2022).
36. Basisty, N. *et al*. A proteomic atlas of senescence-associated secretomes for aging biomarker development. *PLoS Biol.* **18**, e3000599. https://doi.org/10.1371/journal.pbio.3000599 (2020).
37. Ohtani, N. The roles and mechanisms of senescence-associated secretory phenotype (SASP): can it be controlled by senolysis? *Inflamm. Regeneration* **42**. https://doi.org/10.1186/s41232-022-00197-8 (2022).
38. Franceschi, C. *et al*. Inflammaging: a new immune–metabolic viewpoint for age-related diseases. *Nat. Rev. Endocrinol.* **14** (10), 576–590. https://doi.org/10.1038/s41574-018-0059-4 (2018).
39. Ferrucci, L. & Fabbri, E. Inflammageing: chronic inflammation in ageing, cardiovascular disease, and frailty. *Nat. Rev. Cardiol.* **15** (9), 505–522. https://doi.org/10.1038/s41569-018-0064-2 (2016).
40. Zhou, H. *et al*. Colchicine prevents oxidative stress-induced endothelial cell senescence via blocking NF-kappaB and MAPKs: implications in vascular diseases. *J. Inflamm.* **20**. https://doi.org/10.1186/s12950-023-00366-7 (2023).

Acknowledgements

This work was supported by Basic Science Research Program through the National Research Foundation of Korea NRF funded by the Ministry of Education (NRF-2020R1I1A2073643).

Author contributions

H.M. and D.J. contributed equally to this study. Conceptualization: S.W.K. and S.L (Seahyoung Lee); Methodology: H.M., J.-W.C., S.J. and H.K.; Writing original draft: H.M., D.J. and S.W.K.; Reviewing and editing: H.M., B.-W.S., I.-K.K., S.L. (Soyeon Lim) and S.W.K.; Administration: S.W.K.; Funding acquisition: S.W.K.

Declarations

Competing interests
The authors declare no competing interests.

Additional information
Supplementary Information The online version contains supplementary material available at https://doi.org/10.1038/s41598-024-74892-6.

Correspondence and requests for materials should be addressed to S.W.K.

Reprints and permissions information is available at www.nature.com/reprints.

Publisher's note Springer Nature remains neutral with regard to jurisdictional claims in published maps and institutional affiliations.